Deployment of Bistable Self-Deployable Tape Spring Booms Using a Gravity Offloading System

Bistable Tape Spring Booms and Deployment System Design

Bistable tape springs are typically made from high-strength glass fibers or carbon fibers (Herlem 2014; Murphey et al. 2015). Previous experience with tape springs made from woven carbon fibers suggested that tape springs made from glass fibers would provide a good design considering material availability, stored strain energy, and deployed stiffness (Mallol 2013; Mallol and Tibert 2013). In order to have enough deployment energy, i.e., to overcome the matrix energy relaxation, the bistable tape springs were fabricated from four layers of preimpregnated Hexply M77W= 38%=107P=G fabric and the lay directions are [−45F=0F=90F= þ45F], where 0F represents the fabric layer in longitudinal direction (Herlem 2014; Ekelöw 2014). Hexply M77W=38%=107P=G is an epoxy E-glass plain weave prepreg, whereby M77W is the resin type, 38% is the resin content by weight, and the nominal area weight is 107 g=m2 with 53 g=m2 fibers in 0° direction and 51 g=m2 fibers in 90° direction (Hexcel Corporation 2014; Hexcel Corporation 2013). The thickness of each layer is 0.097 mm. The midradius, R, and angle, β, of the cross section circular arc of the 1-m long tape springs are 7.2 mm and 180°, respectively. Material properties were measured by an Instron 5,567 Series machine and three-dimensional (3D) digital image correlation system. The tensile modulus in 0° and 90° directions were E1 ¼ 20 GPa and E2 ¼ 19.5 GPa, respectively. The Poisson's ratio v12 ¼ 0.11 and the shear modulus G12 ¼ 3.5 GPa. Tape spring bistability is given by the outer 45° layers, but as the viscoelastic energy relaxation is attributed to shear strain in the outer 45° layers (Peterson and Murphey 2013) two inner layers 0°=90° are used to mitigate the relaxation effects and increase the deployment force. The laminate was cured at 125°C for 2 h. The tape spring was placed in a vacuum bag with full vacuum (approximately 0 Pa), and the vacuum pump was kept on during the curing process to ensure a smooth outer surface of the tape springs. Thus, through the four-layer-layup the tape springs were designed to mitigate viscoelastic relaxation effects so that the end masses of the boom could be deployed (even after long-term stowage). The bistability criterion indicated that the designed tape springs would not be bistable immediately after fabrication if friction, viscoelastic relaxation, hysteresis, and manufacturing errors

were neglected (Guest and Pellegrino 2006). However, 12 of the 16 tape springs were bistable immediately after fabrication, while four became bistable after being coiled for a few hours. It was observed that the SEAM tape springs (Fig. 2) are straighter compared to the tape spring in Brinkmeyer et al. (2016) that twists approximately 140 degree=m after demolding. One reason is that the plain-weave fabric has approximately the same amount of fibers both in longitudinal and transversal directions compared with the unidirectional fabric in Brinkmeyer et al. (2016), so the laminate is nearly balanced and symmetric and the bending-stretching coupling is nearly zero. This allows fabrication of twist-free tape springs, which are resistant to thermally induced cross section deformations (Peterson and Murphey 2013). The natural coiling radius of the tape springs was 12.5 mm, and they are bistable with a coiling radius between 10 and 15.5 mm [Fig. 2(a)]. The lightweight tape spring, which is approximately 14 g=m [Fig. 2(b)], self-deployed from the coiled to the extended stable state [Fig. 2(c)]. After being stowed for 10 months at room temperature and with an initial coiling radius of 10 mm, the tape springs self-deployed to more than 90% of the length [Fig. 2(d)]. All tape springs in the present study were stored at room temperature with an inner coiling radius of 10 mm. The details of the manufacturing of the tape springs are described in Herlem (2014) and Ekelöw (2014).

Fig. 3 shows a prototype of the stowed SEAM booms assembly based on the patented SIMPLE boom [Murphey et al. 2010; T. W. Murphey et al., "Deployable space boom using bi-stable tape spring mechanism," U.S. Patent No. 8, 770, 522 (2014)]. The booms were composed of four 1-m bistable tape springs that were elastically coiled on two counter rotating spools and stowed in the central hub, mB ¼ 0.230 kg, with a volume of 100 × 80 × 95 mm3. Tip masses (mA ¼ 0.240 kg and mC ¼ 0.255 kg) were fixed on the left and right tip of the booms and deployed simultaneously through the kinematic coupling [Fig. 3(a)]. A 0.39-mm diameter ultrahigh-molecular-weight (UHMW) polyethylene-braided cord was circled around the prototype booms assembly to prevent self-deployment. When the cord was cut the strain energy was released to deploy the end masses. Root-locking tapes and rods [Fig. 3(d)] were used to guide the tape springs during deployment and to make the root of the booms stiffer in bending and torsion.

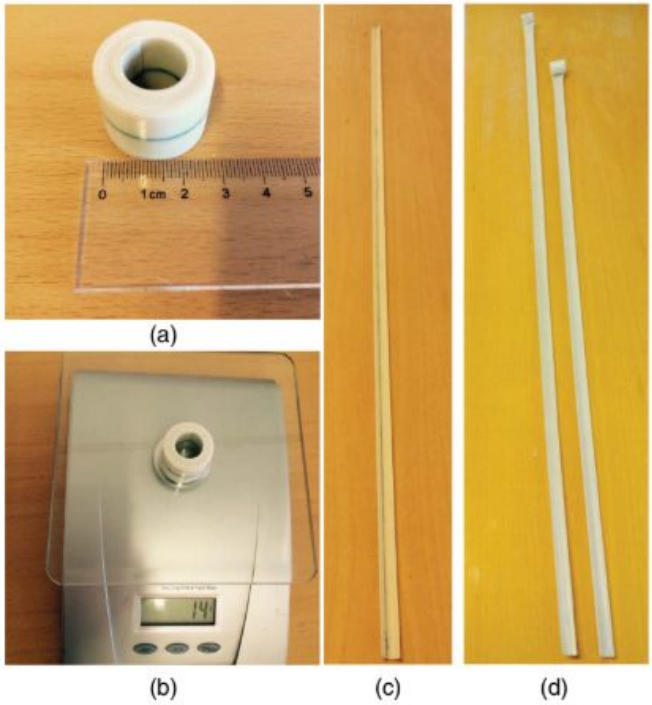

Fig. 2. 1 m glass fiber bistable tape springs: (a) coiled stable state; (b) mass of one tape spring; (c) extended stable state; (d) partially deployed tape springs (image by Huina Mao)

BI-STABLE COMPOSITE SHELLS

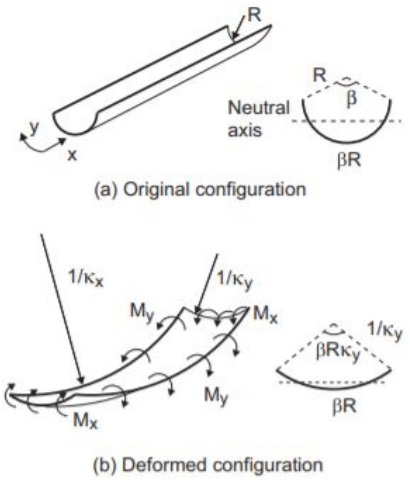

Figure 4: Uniform bending of cylindrical shell.

A simple model for the bi-stability of a shell structure with uniform transverse curvature, $1/R$, that is subjected to uniform curvature changes κ_x and $\kappa_y - 1/R$, Fig. 4, was proposed by Iqbal et al. (1998).

The strain energy in the shell has the expression

$$U = U_b + U_s \tag{3}$$

where the bending and stretching energies have the following approximate expressions

$$\begin{aligned} U_b &= \frac{1}{2}\beta R[D_{11}\kappa_x^2 + 2D_{12}\kappa_x(\kappa_y - \frac{1}{R}) \\ &\quad + D_{22}(\kappa_y - \frac{1}{R})^2] \end{aligned} \tag{4}$$

$$\begin{aligned} U_s &= \frac{A_{11}}{2}[\frac{\beta R}{2}\frac{\kappa_x^2}{\kappa_y^2} + \frac{\sin(\beta R\kappa_y)}{2}\frac{\kappa_x^2}{\kappa_y^3} \\ &\quad - \frac{4\sin^2(\beta R\kappa_y/2)}{\beta R}\frac{\kappa_x^2}{\kappa_y^4}] \end{aligned} \tag{5}$$

Figure 5 shows a contour plot of the total strain energy for a shell with $\alpha = 45°$ as a function of the total curvatures in the longitudinal and transverse directions, κ_x vs. κ_y. The transverse radius of the shell is $R = 25$ mm, and the angle subtended by the cross section is $\beta = 160°$.

As well as having an absolute minimum ($U = 0$) at $\kappa_x = 0$, $\kappa_y = 1/R = 0.04$ mm^{-1}, which be readily verified on the left-hand side inset plot (U vs. κ_y), the plot shows the existence of a local minimum at $\kappa_y \approx 0$ and $\kappa_x \approx 1/36$ mm^{-1}. This local minimum corresponds to the rolled-up configuration of the shell.

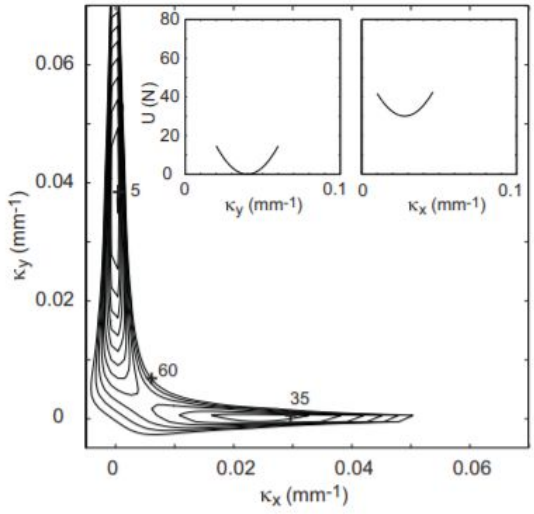

Figure 5: Energy plot for shell with $\alpha = 45°$ and $R = 25$ mm.

This simple model is able to capture the main features of the folding of cylindrical bi-stable shells. However, it is of limited accuracy in predicting the value of the coiled-up radius of the shell: it typically overestimated R by about 20% for $\alpha = 45°$ and by up to 50% for larger values of α. Also, because the model assumes uniform curvature changes, it cannot provide accurate estimates of the peak strain that occurs during coiling; knowing this value is important for design purposes.

Finite Element Modelling

An extensive computational study of bi-stable composite shells was carried out using the finite-element package ABAQUS (Hibbitt et al.,1999). Initially, thin shell elements S8R5 (8 nodes, reduced integration, 5 degrees of freedom per node) were used with the *composite* option to create five layers within the thickness of the shell element. In each layer, of specified thickness, the direction of the fibres was defined by the *orientation* command. This creates a local co-ordinate system for each layer, which in a large displacement analysis rotates with the average rigid body motion of the material point.

The thin shell elements worked well for the moderately non-linear analyses that were carried out at the beginning and which are described next. However, general purpose shell elements, such as S4R (4 nodes, reduced integration), were found to have more robust convergence properties in the heavily non-linear simulations that are described in the section Simulation of Bi-stable Shells.

Linear-elastic behaviour was assumed for each lamina, the material properties being those listed in Table 1.

Table 1: Tape-spring geometry, material systems and associated mechanical properties (1 and 2 refer to the material principal coordinate system, i.e. the fiber directions).

Property	Boom	Antenna	Soft Matrix Antenna
Fiber	T300 Carbon Fiber	E-Glass	E-Glass
Form	Plain Weave	Plain Weave	Plain Weave
Matrix	E765 Epoxy (Park Electrochemical Corp.)	E765 Epoxy (Park Electrochemical Corp.)	Lower modulus material
Fiber Volume Fraction	44 to 54%	42 to 50%	42 to 50%
Thickness	0.127 mm	0.127 mm	0.127 mm
Inner Radius	6.35 mm	6.35 mm	6.35 mm
Section Angle	180 deg	180 deg	180 deg
E_1 and E_2	53.2 GPa	25.5 GPa	25.5 GPa
ε_1^T and ε_2^T	0.97%	1.49%	NA
ε_1^C and ε_2^C	1.19%	1.57%	NA
G_{12}	3.86 GPa	4.83 GPa	2.42 GPa
γ_{12}^F	3.37%	2.71%	NA
ν_{12}	0.059	0.157	0.157
ρ	1,450 to 1,500 kg/m^3	1,760 to 1,870 kg/m^3	NA

Table 2: Tape-spring material system elastic constants with respect to the tape-spring coordinate system (x and y refer to the tape-spring long and transverse axes).

Property	Boom	Antenna	Soft Matrix Antenna
Fiber	T300 Carbon Fiber	E-Glass	E-Glass
E_x and E_y	13.6 GPa	14.6 GPa	8.33 GPa
G_{xy}	25.1 GPa	11.0 GPa	11.0 GPa
ν_{xy}	0.760	0.516	0.725